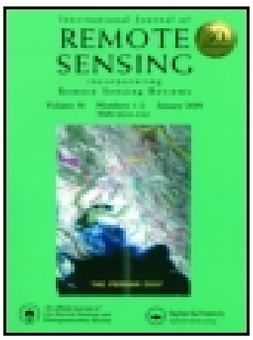

International Journal of Remote Sensing

ISSN: 0143-1161 (Print) 1366-5901 (Online) Journal homepage: https://www.tandfonline.com/loi/tres20

Enhancement of vertical cloud-induced radiative heating in East Asian monsoon circulation derived from CloudSat-CALIPSO observations

Zengxin Pan, Feiyue Mao, Xin Lu, Wei Gong, Huanfeng Shen & Qingzhou Mao

To cite this article: Zengxin Pan, Feiyue Mao, Xin Lu, Wei Gong, Huanfeng Shen & Qingzhou Mao (2019): Enhancement of vertical cloud-induced radiative heating in East Asian monsoon circulation derived from CloudSat-CALIPSO observations, International Journal of Remote Sensing, DOI: 10.1080/01431161.2019.1646935

To link to this article: https://doi.org/10.1080/01431161.2019.1646935

INTERNATIONAL JOURNAL OF REMOTE SENSING
https://doi.org/10.1080/01431161.2019.1646935

Taylor & Francis
Taylor & Francis Group

Enhancement of vertical cloud-induced radiative heating in East Asian monsoon circulation derived from CloudSat-CALIPSO observations

Zengxin Pan[a], Feiyue Mao[a,b,c], Xin Lu[a], Wei Gong[a,c], Huanfeng Shen[d] and Qingzhou Mao[b]

[a]State Key Laboratory of Information Engineering in Surveying, Mapping and Remote Sensing, Wuhan University, Wuhan, China; [b]Department of Remote Sensing, School of Remote Sensing and Information Engineering, Wuhan University, Wuhan, China; [c]Collaborative Innovation Center for Geospatial Technology, Wuhan, China; [d]Department of Geographic Information Science and Mapping, School of Resource and Environmental Sciences, Wuhan University, Wuhan, China

ABSTRACT

Improving the understanding of cloud–radiation–monsoon interactions is difficult due to the limited knowledge regarding the impacts of vertical cloud radiative forcing on monsoon circulation. Here, we focus on the annual cycle of the vertical structure of cloud-induced radiative heating (CRH) to evaluate further their impacts on the East Asian monsoon circulation (100°–140° E, 20°–45° N) derived from satellite observations and reanalysis datasets. Entire troposphere and lower stratosphere are heated by vertical CRH, with the peak reaching 1 K day^{-1} at the mid-level troposphere (4–10 km) during summer. Although radiative warming occurs below 3 km from the prevailing stratocumulus, widespread weak radiative cooling (approximately −0.2 K day^{-1}) occurs at a wide vertical range above 3 km during winter. Consequently, the wind vector variations resulting from vertical CRH highly coincide with the monsoon circulation, leading to the increase in wind speeds by 1.8 and 0.5 m s^{-1} during summer and winter, respectively, while a weakly negative influence (about 0.3 m s^{-1}) occurs at the low-level troposphere below 3 km during winter. Although high clouds, stratiform clouds, and stratocumulus dominate these wind vector variations, deep convective clouds generate the strongest updraft (up to 7 m s^{-1}) amongst all cloud categories despite their low occurrence frequency. Results highlight the important enhancement of vertical CRH to East Asian monsoon circulation by perturbing the vertical structure of heating rate.

ARTICLE HISTORY
Received 29 May 2018
Accepted 19 May 2019

1. Introduction

Clouds crucially regulate atmospheric energy balance, water circulation, and Earth's climate system with multiple spatiotemporal scales (Boucher et al. 2013). Fundamental conundrums on clouds, the coupling of clouds with atmospheric circulation, and climate interactions have remained unsolved and have been identified as considerable challenges in climate research (Bony et al. 2015). One of the largest uncertainties amongst these challenges is the vertical

CONTACT Feiyue Mao maofeiyue@whu.edu.cn State Key Laboratory of Information Engineering in Surveying, Mapping and Remote Sensing, Wuhan University, Wuhan 430079, China

property of clouds and their radiative effects (Li et al. 2015). Vertical variation of clouds can affect the vertical distribution of atmospheric radiative heating, surface energy balance, and general circulation by changing the vertical structure of radiative warming and cooling rates (Johansson et al. 2015; Pan et al. 2017). Quantifying the vertical distribution of cloud radiative forcing and their impacts on atmospheric circulation and regional climate has become critical.

Clouds over East Asia are influenced by monsoon and have become more complicated than those over other regions; as such, these clouds interact with radiation and affect the precipitation pattern and monsoon circulation (Wang et al. 2012). Lu, Yang, and Fu (2016) indicated that stratiform clouds are mostly responsible for the large-scale precipitation over East Asia. Deep convective clouds produce strong radiative and latent heating from the ground surface to the upper troposphere, thereby, considerably affecting atmospheric circulation from the onset to maturity of the summer monsoon (Wang and Wang 2016). High clouds are the most prevalent with substantial seasonal variations over East Asia, and their radiative heating in the upper troposphere region is extensively recognized (Luo, Zhang, and Wang 2009). Cloud–monsoon interaction highly depends on different vertical radiative properties and categories of clouds over East Asia, with summer and winter monsoons prevailing alternately every year.

Several studies have partially determined different total column cloud properties and their radiative effects over East Asia; however, comprehensively investigating the annual cycle of the vertical structure of cloud-induced radiative heating (CRH) and their impacts on regional atmospheric circulation remains lacking (Luo, Zhang, and Wang 2009; Pan et al. 2015; Li et al. 2017). Luo, Zhang, and Wang (2009) previously presented cloud occurrence frequency and vertical location in China by using CloudSat data. Pan et al. (2015) provided a detailed report on the seasonally vertical structure of cloud macrophysical and optical characteristics, but excluded the vertical radiative effects of clouds. Guo et al. (2015) further simulated the total radiative effects of clouds on the East Asian summer monsoon circulation, but did not quantify the contribution of different cloud categories. Given the lack of investigation on the annual evolution of vertical cloud radiative heating or cooling and their impacts on monsoon circulation, the limited knowledge regarding the regional cloud–radiation–monsoon interactions and their parameterizations in climate models have become one of the largest uncertainties requiring solutions to understand potential climate processes and changes.

This study quantifies the annual evolution of vertical cloud–radiation associations and related impacts on the East Asian monsoon circulation derived from satellite observations and reanalysis datasets. The primary motivations are as follows: (1) to investigate the evolution of the vertical structure of CRH within the annual cycle, (2) to quantify the absolute contribution of different cloud categories to total CRH, and (3) to evaluate further the impacts on East Asian monsoon circulation. Resolving these problems is the first step towards comprehending regional clouds, their coupling with atmospheric circulation, and climate interactions and towards quantifying the role of the radiative heating or cooling effects of clouds in regulating the atmospheric circulation and climate over East Asia.

2. Data and methodology

2.1. Data

CloudSat and cloud-aerosol lidar and infrared pathfinder satellite observations (CALIPSO) were launched in April 2006, with primary loads of radar and lidar, respectively (Winker, Hunt, and McGill 2007). Until early April 2011, CloudSat and CALIPSO were maintained in tight orbital coordination as part of the A-train satellite constellation, with the temporal differences between the two satellites kept nominal at 15 s (Mace et al. 2009). Lidar is more sensitive to optically thin cirrus and aerosol than radar, whereas radar is more suitable for probing optically thick clouds because of its wavelength (Mace and Zhang 2014). Therefore, the combined CloudSat and CALIPSO datasets are currently the only available observations that can be used to determine the vertical distribution of clouds and aerosols and obtain information regarding their type and phase with high confidence (Winker et al. 2010; Pan et al. 2018). Various studies, which combine cloud masks from the millimetre-wave radar on CloudSat and lidar on CALIPSO, have been conducted to investigate the three-dimensional properties of clouds at regional and global levels (Guo et al. 2016; Lu et al. 2018; Liu et al. 2018).

We analysed the vertical structure of CRH and the related contributions of different cloud categories over East Asia by using the combined CloudSat and CALIPSO products of 2B-CLDCLASS-LIDAR and 2B-FLXHR-LIDAR R04 from 2006 to 2010. The combined products have a 1.3 km cross-track and 1.7 km along-track footprint resolutions, and the effective vertical resolution at nadir is 240 m (Stephens et al. 2008). The 2B-FLXHR-LIDAR simulates the radiative effects of cloud and aerosol by using a broadband two-stream doubling–adding radiative transfer model (BUGSrad) and assuming a plane-parallel atmosphere (Fu and Liou 1992; Henderson et al. 2013). This model is based on the retrieved profiles of the macro- and microphysical properties of cloud and aerosol from CloudSat and CALIPSO. Information regarding the atmospheric state variables was obtained from the analysis results of the European Centre for Medium-Range Weather Forecasts-Auxiliary (ECMWF-AUX; Dee et al. 2011). The detailed algorithm of CloudSat 2B-FLXHR-LIDAR was reported by L'Ecuyer et al. (2008) and Henderson et al. (2013).

Henderson et al. (2013) stated that the global mean outgoing shortwave (SW) and longwave (LW) radiations from 2B-FLXHR-LIDAR have collocated with the Clouds and the Earth's Radiant Energy System (CERES) observations and are consistent within 4 W m^{-2} (less than 4%) and 5 W m^{-2} (approximately 2%) on monthly/5° scales, respectively. The heating rates (HRs) of SW and LW have recorded errors of 12.5% at the global level (Haynes et al. 2013; Mao et al. 2018). The root mean square errors of SW and LW HRs are 4% and 7%, respectively, when directly comparing gridded column HRs between CERES and 2B-FLXHR-LIDAR. Moreover, the uncertainties of radiative fluxes derived from 2B-FLXHR-LIDAR considerably decrease for longer timescale averages (L'Ecuyer et al. 2008). In summary, these data can be considered credible for investigating the SW and LW radiative effects of clouds over East Asia.

2.2. Methodology

The 2B-CLDCLASS-LIDAR product can classify clouds into high (above 7 km), altostratus, altocumulus, stratus, stratocumulus, cumulus, nimbostratus, and deep convective clouds on the basis of cloud base height and horizontal properties, the presence or absence of precipitation, cloud temperature, and upward radiance from Moderate Resolution Imaging Spectroradiometer measurements (Sassen, Wang, and Liu 2008). Cloud–aerosol mask inspection show that layers are appropriately identified with approximately 90% accuracy (Sassen, Wang, and Liu 2009). The present study used the 2B-CLDCLASS-LIDAR data product to quantify the categories and related vertical frequency of clouds with high significance, which was calculated by dividing the number of cloudy pixels of a particular cloud type by the total number of pixels at each height bin.

As polar orbit satellites, CloudSat and CALIPSO, obtain atmospheric profiles only at certain times of the day at each location. The instantaneous observations of SW HR from 2B-FLXHR-LIDAR are considerably more than the daily average HR at all times. Therefore, SW HR is normalized by a factor that considers the diurnal variation of incident solar radiation. The normalization factor is computed using Equation (1):

$$r_F = F^{\downarrow} \Big/ \overline{F}^{\downarrow}, \tag{1}$$

where $\overline{F}^{\downarrow}$ and $F^{\downarrow}$ are the daily average and observed instantaneous solar radiations at the top of the atmosphere, respectively. $\overline{F}^{\downarrow}$ is calculated using the method presented by Quaas et al. (2008). For a particular cloud type, the related net CRH is the sum of SW and LW CRH and is calculated using the method proposed by Johansson et al. (2015), as shown in Equation (2):

$$\mathrm{CRH} = (r_F \times (Q^{\mathrm{SW}}_{\mathrm{Cloudy}} - Q^{\mathrm{SW}}_{\mathrm{Clear}}) + (Q^{\mathrm{LW}}_{\mathrm{Cloudy}} - Q^{\mathrm{LW}}_{\mathrm{Clear}})) \times \mathrm{CF}, \tag{2}$$

where $Q^{\mathrm{SW}}_{\mathrm{Cloudy}}$ and $Q^{\mathrm{SW}}_{\mathrm{Cloudy}}$ are the SW and LW HR vectors under a cloud-sky condition, respectively. By contrast, $Q^{\mathrm{SW}}_{\mathrm{Clear}}$ and $Q^{\mathrm{SW}}_{\mathrm{Clear}}$ are the SW and LW HRs vectors under a clear sky condition, respectively. The absolute contribution of this particular cloud type was obtained by weighing the related absolute cloud fraction (CF).

Atmospheric heating from clouds is generally balanced by thermodynamic adiabatic cooling through vertical upward motion; thus, monsoon circulation is distinctly affected by this vertical thermodynamic perturbation (Mather et al. 2007; Guo et al. 2015). This phenomenon can be explained by applying the following simplified thermodynamic energy equation:

$$\omega \frac{\boldsymbol{N}^2 \boldsymbol{H}}{\mathrm{R}} = \boldsymbol{Q}, \tag{3}$$

where R is the gas constant, $\boldsymbol{\omega}$ is the vertical velocity vector, and $\boldsymbol{H}$ and $\boldsymbol{Q}$ represent the scale height and atmospheric HR vectors (Mather et al. 2007). The Brunt–Vaisala frequency ($\boldsymbol{N}^2$) is a widely used dynamical vector that determines atmospheric stratification and defined as follows:

$$N^2 = \frac{g}{\boldsymbol{T}_\theta} \frac{\partial \boldsymbol{T}_\theta}{\partial \boldsymbol{z}}, \tag{4}$$

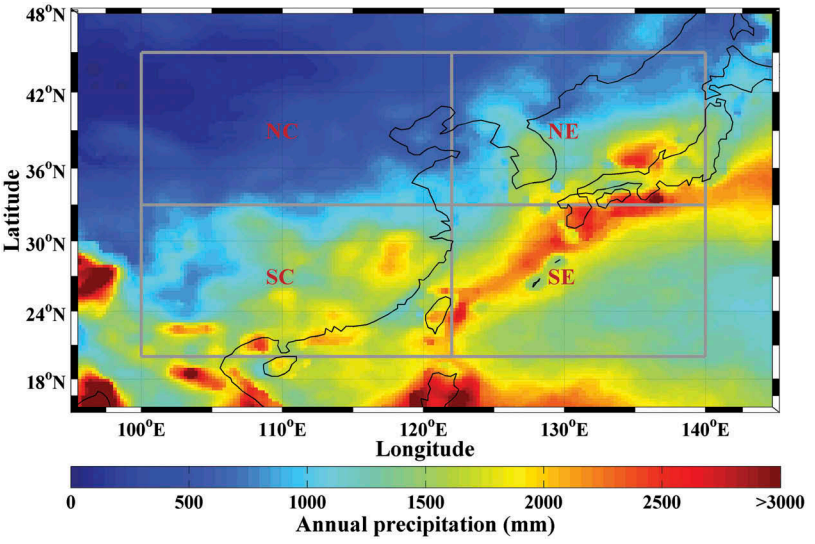

Figure 1. Annual average total precipitation from 1998 to 2014 over East Asia. The grey lines represent the boundary of sub-regions in this study.

where g is the local acceleration constant due to gravity, $\boldsymbol{T}_\theta$ and $\boldsymbol{z}$ are the potential temperature and height vectors, and $\partial \boldsymbol{T}_\theta / \partial \boldsymbol{z}$ is the potential temperature gradient (Wu et al. 2015). Therefore, the impacts of CRH on locally vertical atmospheric motions are evaluated as the difference of $\boldsymbol{\omega}$ under all sky and clear sky conditions.

Figure 1 presents the annual average total precipitation from the Tropical Rainfall Measuring Mission (Henderson et al. 2017). The total precipitation gradually decreases with the weakened summer monsoon from southern to northern East Asia. Moreover, precipitation over the sea is more than that over land and is focused on the southeast (SE) islands of East Asia. Therefore, we divided East Asia into Southern Continent (SC; 100–122° E, 20–33° N), Northern Continent (NC; 100–122° E, 33–45° N), SE (122–140° E, 20–33° N), and northeast (NE; 122–140° E, 33–45° N) by considering the differences in their precipitation, climate, and underlying surface to determine the differences in the vertical structure of CRH in different regions of East Asia accurately (Ding, Wang, and Sun 2008; Ding and Chan 2005).

3. Results and discussion

3.1. Monthly evolution of the vertical structure of clouds

The monthly evolution of the average vertical occurrence frequency of clouds over East Asia indicates vertical variations of clouds triggered by monsoon circulation (Figure 2). The seasonal cloud amount reaches its maximum value during summer (particularly in southern East Asia), with the southerly summer monsoon winds transporting a considerable amount of precipitation (Ding and Chan 2005). The cloud amount over East Asia exhibits a sharp decrease during autumn after the southerly summer monsoon retreats and the northerly winter monsoon is generated, with a gradual weakening of

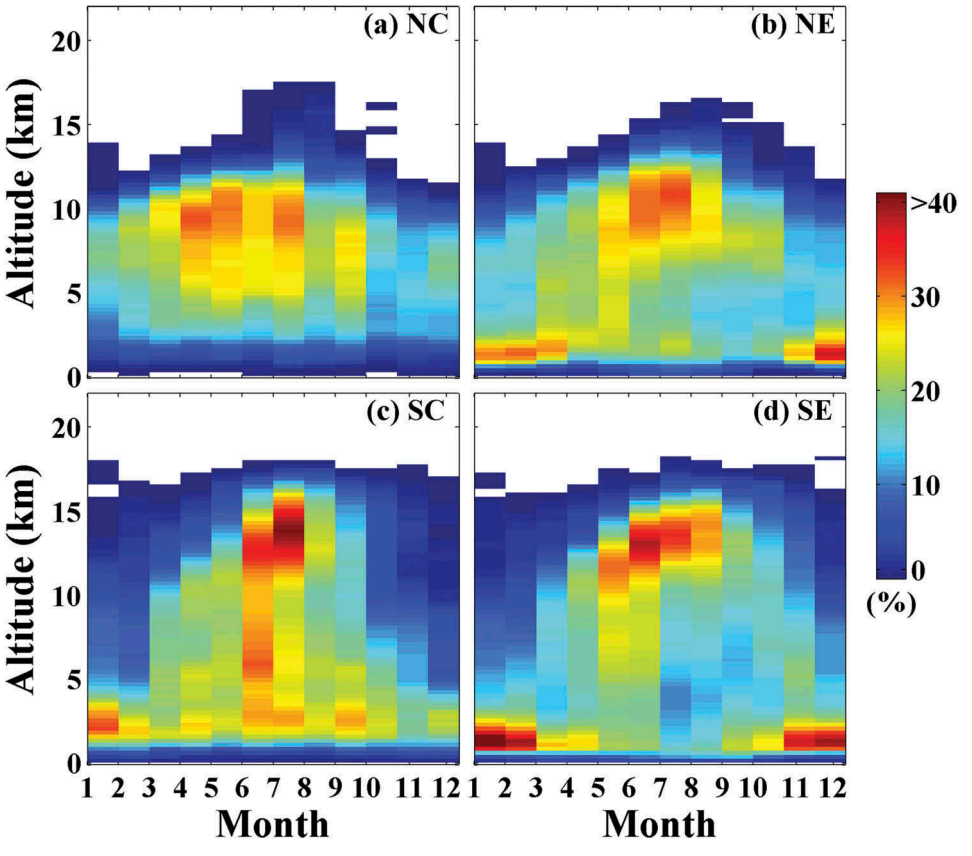

Figure 2. Monthly evolution of the average vertical frequency of clouds over the sub-regions within East Asia from 2006 to 2010: (a) NC; (b) NE; (c) SC; and (d) SE. The blank indicates a fairly low occurrence frequency (less than 0.1%) at the height bin.

vertical convection and a decrease in water vapour (Ding et al. 2014). Given that summer and winter monsoons alternately prevail every year, we observe general seasonal variations in which clouds appear the most and the highest during summer and the least and the lowest during winter across the four seasons over East Asia. In addition, more distinct seasonal variations of the vertical frequency of clouds occur over southern East Asia than that over northern East Asia, where clouds are mostly concentrated at an altitude of 5–10 km throughout the year.

Different cloud types play a unique role in the cycle of summer and winter monsoons; such role results from their radiative heating or cooling capacity and the latent heat released from precipitation (Rosenfeld et al. 2014). For example, stratiform clouds distinctly contribute to a substantial amount of rainfall covering large areas of East Asia (Lu, Yang, and Fu 2016). Deep convective clouds are considerably related to strong convective precipitation and produce strong latent heating, which can sustain monsoonal circulation during summer. Moreover, Table 1 shows that high clouds dominate the cloud systems during summer, whereas stratocumulus and altocumulus are dominant during winter with a summed probability of 46.7% and substantial seasonal variations. Therefore, we divide all cloud layers into five cloud categories associated with

Table 1. Statistics of annual and seasonal average probability for different cloud categories over East Asia from 2006 to 2010 (unit: %).

	Annual	Spring	Summer	Autumn	Winter
High clouds	31.5	32.5	44.5	25.8	15.2
Stratiform	20.3	24.8	12.5	18.7	28.5
Stratocumulus	18.1	15.6	10.7	20.7	31.2
Cumuliform	28.3	25.7	29.2	33.1	24.7
Deep convective	1.8	1.4	3.1	1.7	0.4

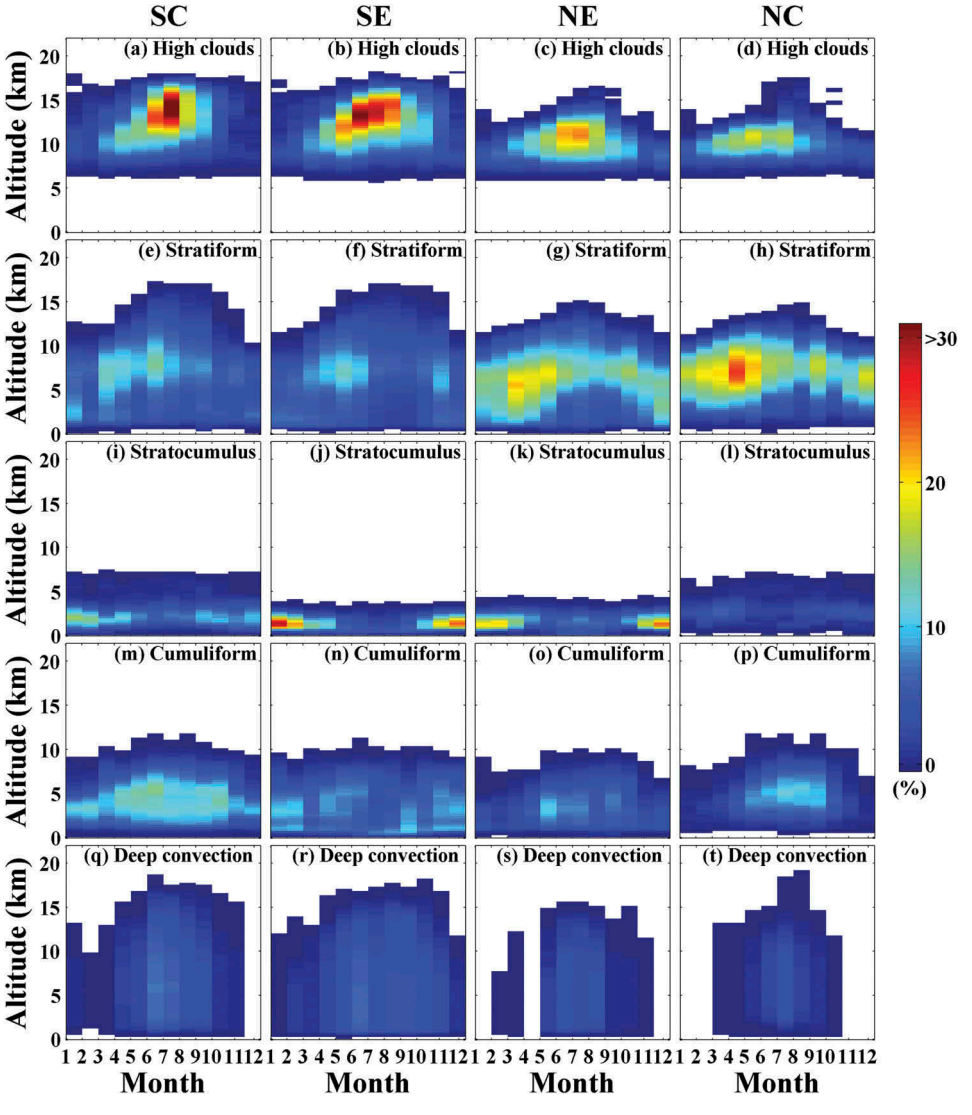

Figure 3. Monthly evolution of the average vertical frequency of different cloud categories over the sub-regions within East Asia from 2006 to 2010: (a–d) high, (e–h) stratiform, (i–l) stratocumulus, (m–p) cumuliform, and (q–t) deep convective clouds. The blank indicates a fairly low occurrence frequency (less than 0.1%) at the height bin.

precipitation and distinct seasonal variations to investigate the related contributions of different cloud categories to the vertical structure of CRH (Johansson et al. 2015). These cloud categories are high, stratiform (altostratus, stratus, and nimbostratus), stratocumulus, cumuliform (altocumulus and cumulus), and deep convective clouds.

High clouds prevail in the upper troposphere and lower stratosphere (above 10 km), particularly during summer. Moreover, Figure 3(e–l) shows that stratiform clouds and stratocumulus dominate the middle and low cloud systems over East Asia, respectively. Stratiform clouds frequently prevail during spring in northern East Asia (NE and NC), particularly over the NC (occurrence frequency nearly 30%). Stratocumulus becomes increasingly important during spring and winter, particularly over southern East Asia (SC and SE). The aforementioned regional variations indicate that the stratiform clouds are more important than the stratocumulus over northern East Asia, and vice versa over southern East Asia. Cumuliform clouds are prevailing during summer and autumn with the weakest seasonal variations. Furthermore, deep convective clouds occur in the entire troposphere and lower stratosphere and are considerably enhanced by the summer monsoon (Figure 3(q–t)), whereas their occurrence frequency is low.

3.2. Monthly evolution of vertical CRH

Given the distinct annual cycle of the absolute vertical frequency of clouds, investigating the corresponding monthly variations of CRH provides interesting insights to evaluate directly the interaction between vertical CRH and regional atmospheric circulation (Johansson et al. 2015). When a cloud layer occurs, the atmospheric column can be heated due to the absorption and scattering of solar radiation by clouds. This scene commonly generates SW heating within and above the cloud layer, which decreases incident solar radiation at the cloud base. Simultaneously, clouds distinctly absorb LW radiation emitted from the surface, which causes LW heating within and under the cloud layer, thereby decreasing LW radiation at the cloud top and further resulting in LW cooling above the cloud.

SW heating is highly consistent with the vertical frequency of clouds (Figure 2), with the highest values of more than 0.5 K day^{-1} over all the subregions of East Asia. Simultaneously, weak atmospheric cooling occurs under cloud layers at a magnitude of −0.3 K day^{-1} due to enhanced SW reflection from the clouds. Figure 4(a–d) shows that the monthly variations in SW CRH are also associated with incident solar radiation, which generally reaches its maximum value during summer in the mid-latitudes of the northern hemisphere (Gao, Sui, and Hu 2014). Furthermore, LW radiative forcing in the atmosphere occurs from heating to cooling with altitude due to the variable LW absorption of clouds (Figure 4(e–h)). Robust LW radiative heating occurs in the low-level troposphere (below 4 km) because of the strongest absorption of LW radiation by the clouds emitted from the surface. This phenomenon further causes LW radiative cooling in the high-level atmosphere due to the reduced cloud LW emission at the cloud top, particularly during winter. However, weak LW heating occurs in the upper troposphere (above 10 km) during summer over SC and SE; this phenomenon is attributed to the LW radiation absorbed by the prevailing high clouds during summer (Henderson et al. 2013; Pan et al. 2015).

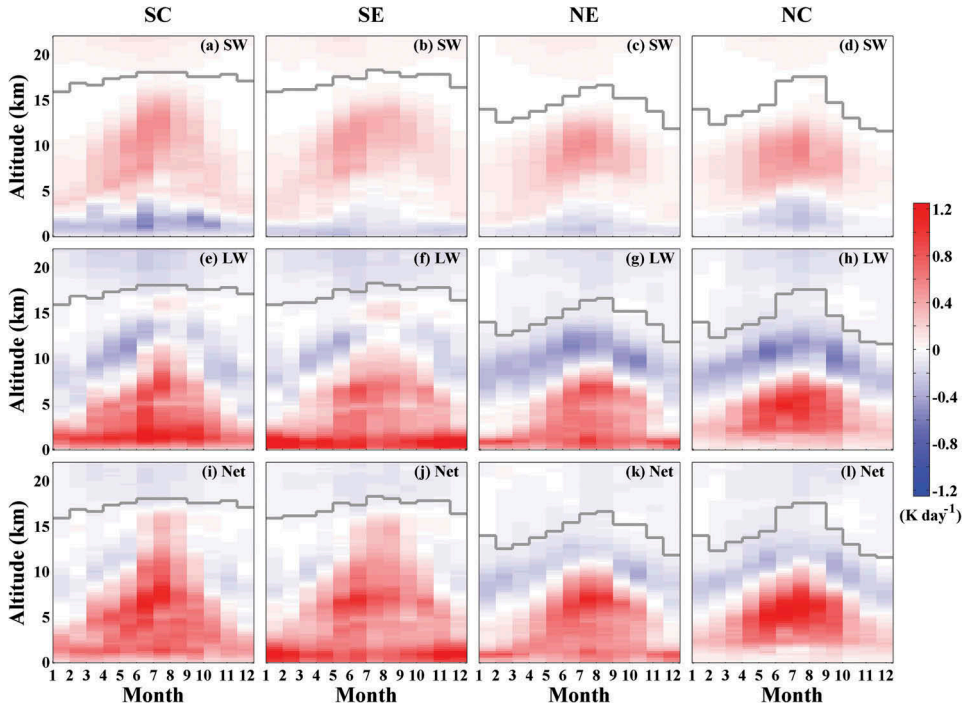

Figure 4. Monthly evolution of average (a–d) SW, (e–h) LW, and (i–l) net CRH of total cloud layers over the sub-regions of East Asia from 2006 to 2010. The grey lines indicate the upper boundary of vertical occurrence range of cloud corresponding to Figure 2.

Clouds generally heat the entire troposphere and the lower stratosphere over East Asia at a maximum of 1.0 K day^{-1} in the mid-level troposphere (4–10 km) during summer due to the resulting strong SW and LW radiative absorptions (Figure 4(i–l)). However, net radiative cooling occurs above the cloud top at a magnitude of lower −0.2 K day^{-1} due to reduced LW emission. The seasonal and regional variations of vertical CRH are determined by the vertical structure of clouds (Johansson et al. 2015; Li et al. 2015). A widespread weak radiative cooling occurs (approximately −0.2 K day^{-1}) at a wide vertical range above 3 km during winter when the clouds nearly concentrate on the lower troposphere. Furthermore, LW CRH dominates the overall vertical radiative effects from clouds, whereas SW CRH occurs in the mid- and high-level troposphere at a magnitude lower than that of LW CRH. This finding is consistent with that of a previous study of Johansson et al. (2015).

Figure 5 shows the evaluated related contributions from different cloud categories to vertical net CRH by considering their absolute vertical occurrence frequency. Quantifying the vertical CRH of a particular cloud category above and under cloud layers is difficult due to cloud overlap (Li et al. 2015). Therefore, we evaluated the vertical CRH of a particular cloud category on the basis of the scenes of single-layer clouds to suppress uncertainties from cloud overlap. The single-layer clouds contribute to two-thirds of the total cloud layers, and their vertical CRH pattern is more consistent with that of the total cloud layers than that of the multilayer clouds (not shown).

High clouds dominate the CRH in the upper troposphere and lower stratosphere (Sassen, Wang, and Liu 2008), particularly over southern East Asia (SC and SE). The

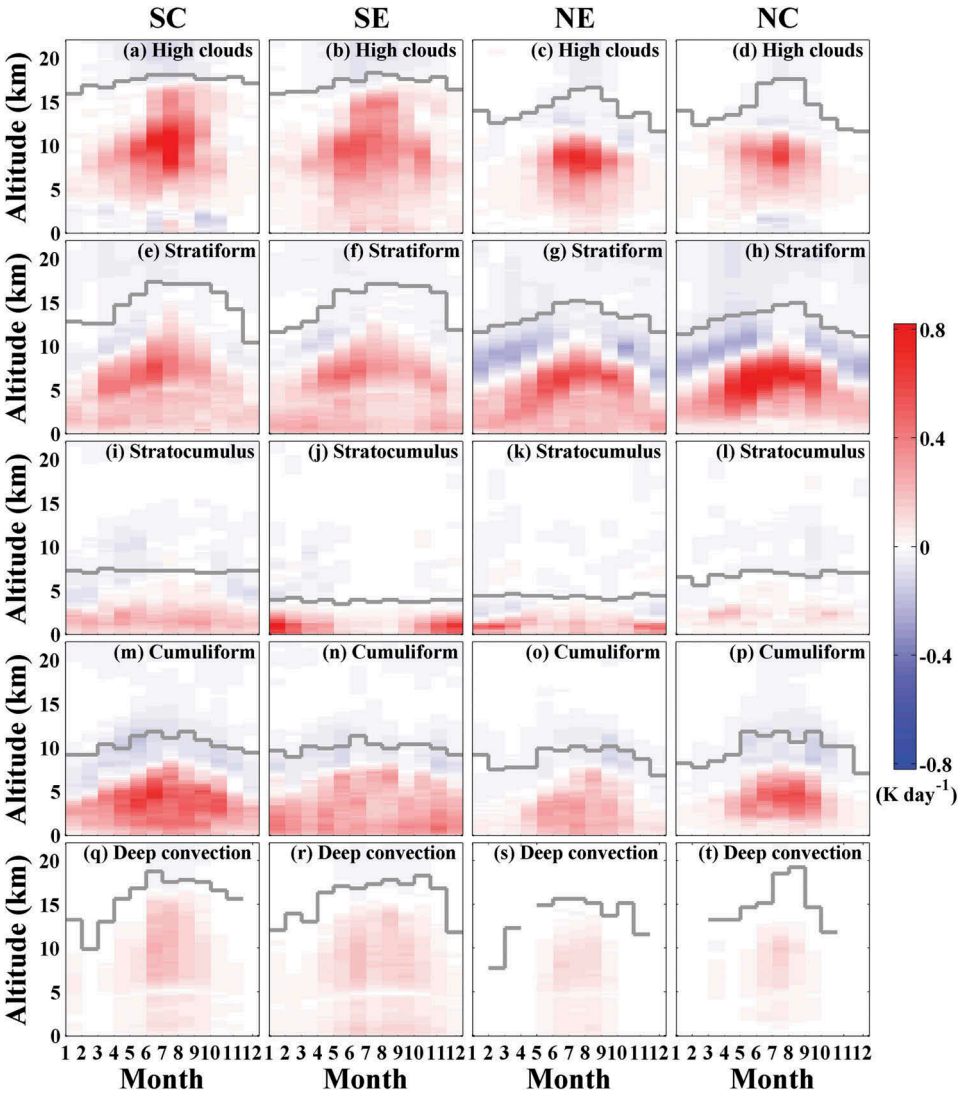

Figure 5. Monthly evolution of average net CRH of all selected cloud categories over the sub-regions of East Asia from 2006 to 2010: (a–d) high, (e–h) stratiform, (i–l) stratocumulus, (m–p) cumuliform, and (q–t) deep convective clouds. The grey lines indicate the upper boundary of vertical occurrence range of all selected cloud categories corresponding to Figure 3.

maximum heating of the CRH (about 0.8 K day^{-1}) occurs during summer because of the prevalence of high clouds (Figure 5(a–d)). Although deep convective clouds are infrequent (Figure 3(q–t)), they generally contribute to the net radiative heating (up to 0.2 K day^{-1}) from the near surface to the upper troposphere (Figure 5(q–t)) in some areas from the surface to 15 km, particularly during summer. High clouds result either from a convective process or a large-scale vertical ascent (Sassen, Wang, and Liu 2009). This condition nearly coincides with the seasonal pattern of CRH by deep convective and high clouds, thereby indicating greater control of high cloud formation through

enhanced convective processes than by large-scale ascent during the summer monsoon (Ding, Wang, and Sun 2008). Furthermore, cumuliform clouds result in the moderate CRH (about 0.5 K day^{-1}) between 2 and 6 km with the consistent seasonal variations as high and deep convective clouds.

Stratiform clouds and stratocumulus dominate the CRH in the mid- and low-level troposphere, respectively, which is consistent with the results in Figure 3. The strongest radiative heating from stratiform clouds (up to 0.8 K day^{-1}) is observed in the mid-level troposphere during summer because of the most prevalent stratiform clouds over NC. Moreover, stratiform clouds result in distinct net radiative cooling (over −0.2 K day^{-1}) in the high-level atmosphere, which is responsible for the net radiative cooling from the total cloud layers (Figure 4(e–h)). Notably, radiative cooling from stratiform clouds is considerably counteracted by warming above 10 km during summer; this phenomenon occurs because of the high vertical variability of these clouds and the additional absorption of cloud layers to SW and LW radiation during summer (Johansson et al. 2015). Furthermore, stratocumulus becomes increasingly important (up to 0.7 K day^{-1}) in the low-level troposphere below 4 km because of the prevailing stratocumulus during spring and winter over southern East Asia (Figure 5(i–l)).

3.3. Enhanced monsoon circulation by vertical CRH

Clouds distinctly regulate vertical atmospheric HRs due to cloud–radiation interaction (Henderson et al. 2013). These atmospheric heating variations from clouds are generally balanced by thermodynamic adiabatic cooling through vertical upward motion variations, which results in distinct impacts on the locally vertical monsoon circulation (Mather et al. 2007; Guo et al. 2015). Figure 6 exhibits the resulting vertical velocity variations from CRH on the basis of thermodynamic balance to quantify the impacts of CRH on the vertical summer and winter monsoon circulations. During summer, the vertical upward motion is enhanced by CRH by approximately −6 hPa day^{-1} at 6–10 km (Figure 6(a)). However, the weak subsidence is approximately 3 hPa day^{-1} in the low-level troposphere (below 3 km) due to the atmospheric cooling that results from the enhanced SW reflection by clouds. Moreover, clouds warm the atmosphere within and below the cloud layers due to LW absorption, thereby enhancing the vertical upward motion at a higher magnitude of approximately −8 hPa day^{-1} than that from SW CRH during summer (Figure 6(a,b)). The atmosphere within and above the cloud top is cooled due to reduced LW emission, which results in atmospheric subsidence at a wide range above 10 km during summer. Furthermore, the vertical motion variations resulting from CRH are contributed by LW CRH.

With the additional heating source, clouds distinctly enhance the vertical upward motions from the near surface to the tropopause, with its peak reaching −10 hPa day^{-1} approximately at the mid-level troposphere (4–10 km) during summer due to SW and LW absorptions. This finding coincides well with the vertical summer monsoon circulation with a dominant large-scale updraft of approximately −20 hPa day^{-1} over East Asia (Figure 6(d)). This finding is consistent with that of the study of Guo et al. (2015) on the basis of a climate model. The impacts of CRH on the vertical motions of the winter monsoon are more complicated than those of the summer monsoon. During winter, robust subsidence reaches up to 40 hPa day^{-1} and controls large-scale atmospheric

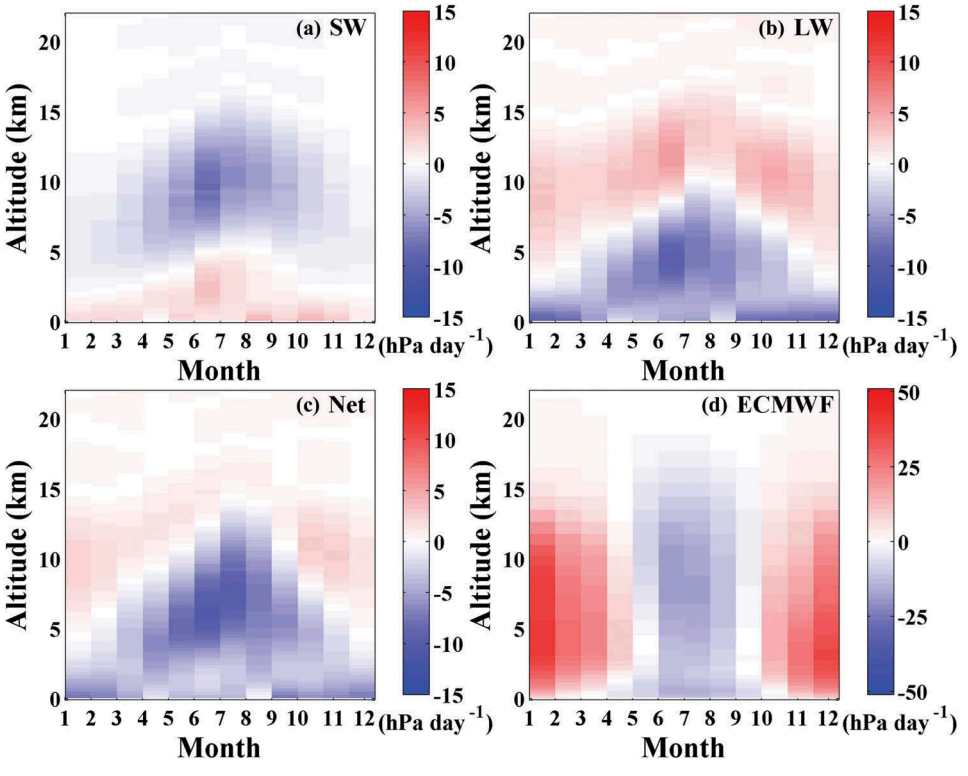

Figure 6. Monthly evolution of average vertical velocity induced by (a) SW, (b) LW, and (c) net CRH, and derived from (d) ECMWF over East Asia from 2006 to 2010.

vertical motions with the prevailing winter monsoon. The weakly enhanced upward motions from CRH constrain the vertical downward motions through the winter monsoon circulation below 3 km with an average of −3 hPa day^{-1}. However, wide subsidence from clouds (about 2 hPa day^{-1}) occurs at a wide range above 3 km due to the reduced LW emission, which coincides well with the vertical downdraft of the winter monsoon over East Asia.

Furthermore, atmospheric vertical motion variations from CRH are generally followed by the meridional wind variations, which can be explained by Sverdrup vorticity balances (Rodwell and Hoskins 2001; Guo and Zhou 2015), using follows Equation (5):

$$\beta \boldsymbol{v} = f \frac{\partial \boldsymbol{\omega}}{\partial \mathbf{p}}, \tag{5}$$

where f and β are the Coriolis parameter and its meridional gradient, respectively. $\partial\boldsymbol{\omega}/\partial\boldsymbol{p}$ is the vertical velocity gradient, which determines the meridional wind based on the Sverdrup vorticity balance. The negative and positive $\boldsymbol{v}$ indicate southward and northward wind vectors, which frequently occur above and under the maximum centre of $\partial\boldsymbol{\omega}/\partial\boldsymbol{p}$, respectively. Figure 7(a,b) shows the latitude–altitude wind vector during summer and winter over East Asia with the shading of the vertical frequency of clouds, respectively. The peak of occurrence frequency (more than 50%) is matched with the maximum vertical updraft during summer and located within the latitude–altitude range of 10–20° N and 10–18 km

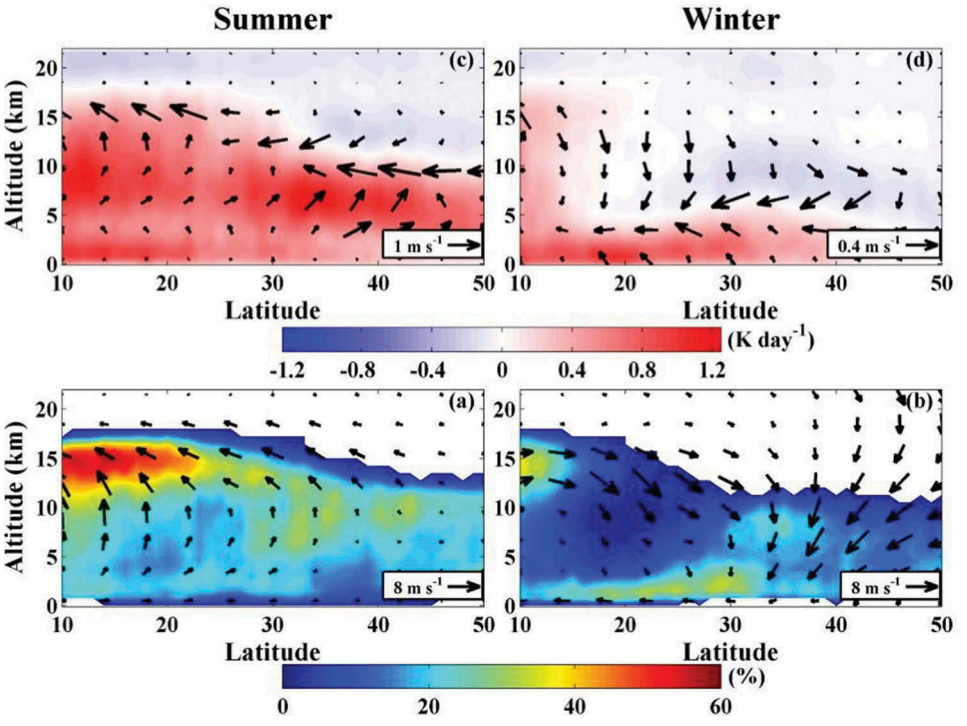

Figure 7. Latitude–altitude wind vectors from ECMWF with the cloud vertical frequency (shading) during (a) summer and (b) winter. The latitude–altitude wind vector variations resulting from vertical CRH (shading) during (c) summer and (d) winter over East Asia from 2006 to 2010.

(Figure 7(a)). Thus, the vertical updraft enhances cloud formation and growth during summer (Luo, Zhang, and Wang 2009). Moreover, clouds concentrate on the location of a wind point at all times, such as the high- and low-level troposphere, during summer and winter (Figure 7(a,b)), respectively. In summary, the vertical structure of clouds is shaped by monsoon circulation over East Asia, particularly the summer monsoon circulation.

Figure 7(c,d) shows that the wind vector variations resulting from CRH are generally consistent with the East Asian monsoon circulation. Clouds generally heat the entire troposphere and the lower stratosphere during summer, thereby strengthening the vertical upward motion and enhancing the northward wind in the low- and mid-level troposphere and southward wind in the high-level troposphere. Thus, vertical CRH considerably enhances the summer monsoon circulation with a maximum wind speed variation of up to 1.8 m s^{-1}, which is consistent with the study of Guo et al. (2015). In addition, low-level clouds dominate the cloud system during winter when robust subsidence controls the atmospheric motion, thereby heating the low-level troposphere, whereas the higher-level troposphere is widely cooled. Consequently, atmospheric subsidence is strengthened and the southward wind is enhanced during winter (up to 0.5 m s^{-1}) at a wide range above 3 km, while the atmospheric subsidence is moderately suppressed by the CRH (about 0.3 m s^{-1}) at the low-level troposphere below 3 km. In addition, the robustness and magnitude of wind vector variations from CRH during winter are lower than those during summer. Generally,

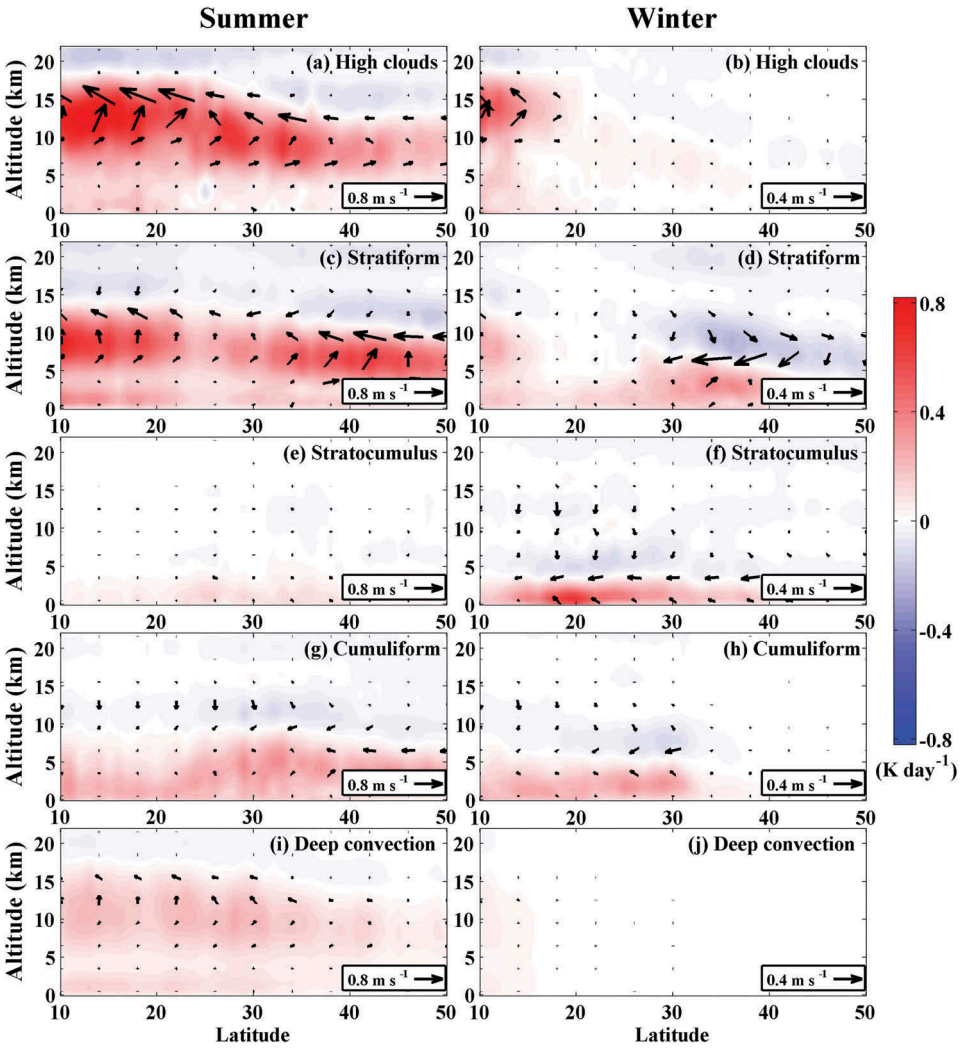

Figure 8. Latitude–altitude wind vector variations resulting from vertical CRH (shading) of all selected cloud categories during summer and winter over East Asia from 2006 to 2010: (a–b) high, (c–d) stratiform, (e–f) stratocumulus, (g–h) cumuliform, and (i–j) deep convective clouds. The blank indicates a fairly low cloud cover (less than 0.1%).

the vertical structure of CRH is favourable to the East Asian monsoon circulation, particularly the summer monsoon circulation.

We further evaluate the related contribution of cloud categories to monsoon circulation variation resulting from the total vertical CRH (Figures 8 and 9). The high-level troposphere (>10 km) is heated by high clouds, thereby inducing large-scale air upwards into the stratosphere and southward to the tropical region during summer (up to 1.2 m s^{-1}). Moreover, stratiform clouds and stratocumulus result in the wind vector variations in the mid- and low-level troposphere, which correspond to the related vertical structure of CRH. Although the stratocumulus (below 3 km) dominantly results in the weakly enhanced upward motion in the low-level troposphere during winter, the wind vector variations

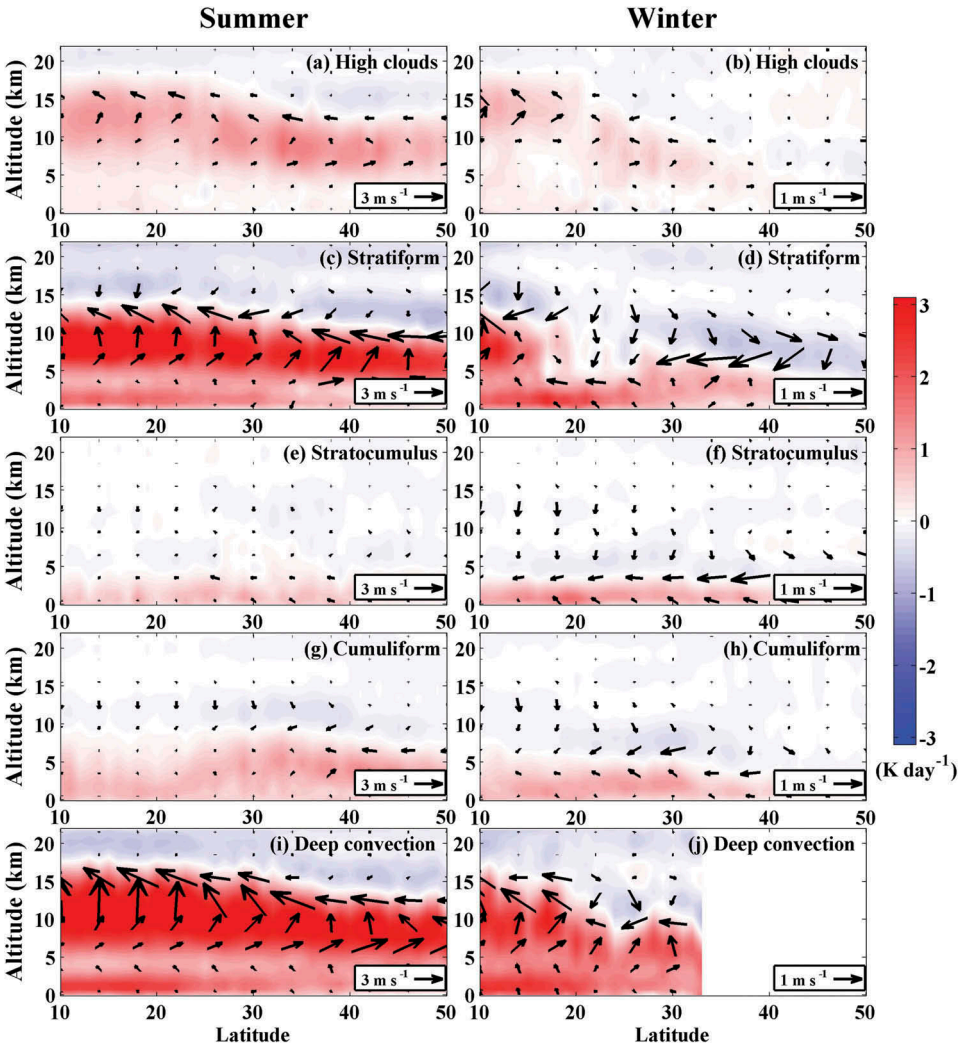

Figure 9. As same to Figure 8, but under the cloud-sky condition.

caused by vertical CRH coincide with the winter monsoon circulation in the higher-level troposphere. The impact of deep convective clouds on monsoon circulation is seemingly negligible, which can be attributed to the low occurrence frequency of these clouds.

The impact of cloud categories on monsoon circulation is a function of cloud occurrence frequency, albeit a distinct difference exists amongst cloud categories (Johansson et al. 2015). For example, high clouds contribute to approximately one-third of the cloud layers, whereas deep convective clouds account for less than 2% over East Asia. Figure 9 indicates that deep convective clouds generate the strongest upward wind vector variations (up to 7 m s^{-1}) under the cloud-sky condition due to its strong radiative absorption, followed by stratiform clouds (up to 5 m s^{-1}), particularly during summer with the intensive atmospheric convection. The related impacts of high clouds are considerably weaker than those of deep convective clouds in terms of magnitude and opposite to that shown in Figure 8. This phenomenon

demonstrated the significant role of deep convection on regulating energy and wind vectors in the entire troposphere, albeit their occurrence frequency is low. Furthermore, stratocumulus and stratiform clouds determine the vertical structure of CRH during winter over East Asia and further generate the wind vector variations coinciding with the winter monsoon circulation, albeit the part inconsistence at the low-level troposphere below 3 km.

3.4. Discussion

This study highlight the impact of the vertical structure of CRH on monsoon circulation derived from satellite observations and reanalysis datasets. The synergy between CloudSat and CALIPSO provides the most comprehensive descriptions for the vertical structure of CRH (L'Ecuyer et al. 2008; Mace and Zhang 2014). Given the limitation of satellite observation for controlling specific atmospheric variations, quantifying further mutual-coupled feedback, and other processes between vertical CRH and monsoon circulation is difficult. Actually, clouds substantially influence the energy budget of the atmosphere at a bigger magnitude when comprehensively considering radiative heating/cooling and latent heat release processes (Zuluaga, Hoyos, and Webster 2010; Johansson et al. 2015). The latent heating associated with precipitation importantly affects the air transmission, especially at the low- and mid-level troposphere (Zuluaga, Hoyos, and Webster 2010). Johansson et al. (2015) also present the importance of CRH significantly increase in upper troposphere where the influence of latent heating is weak. It is worth to further discuss the latent heating process and the related effect on monsoon circulation in the future.

Previous studies have investigated the radiative effects of clouds and their impacts on summer monsoon circulation, but not for the annual cycle of cloud radiative forcing and contribution of different cloud categories (Guo et al. 2015; Johansson et al. 2015; Li et al. 2017). The present results indicate that the vertical structure of CRH is considerably formed by summer and winter monsoons prevailing alternately every year (Luo, Zhang, and Wang 2009; Pan et al. 2015). With the strong upward convective action during summer, the prevailing high and stratiform clouds dominate the radiative heating in the upper and middle troposphere. However, dominant atmospheric subsidence during winter results in the collection of cloud in the lower troposphere (below 3 km) as stratocumulus over East Asia. Wind vector variations caused by vertical CRH generally coincide with the winter monsoon circulation at a wide range above 3 km, while the stratocumulus moderately suppresses atmospheric subsidence in the low-level troposphere during winter. Therefore, the vertical CRH positively affects the East Asian monsoon circulation, particularly during the summer monsoon, in which the robustness and intension of enhancement are higher than that during winter.

4. Conclusion

Clouds are intrinsically associated with radiative balance and they further regulate regional atmospheric circulation. Here, we investigate the annual evolution of the vertical structure of radiative heating induced from different cloud categories and further quantify their impacts on the East Asian monsoon circulation (100–140° E, 20–45° N). We summarize the most important features as follows:

(1) Vertical CRH enhances the vertical updraft from the surface to the lower stratosphere, with the peak reaching −10 hPa day^{-1} (CRH up to 1 K day^{-1}) within 4–10 km during summer and is distinctly contributed by high clouds (44.5%). Although the enhanced updraft at −3 hPa day^{-1} results from the prevailing stratocumulus (31.2%) below 3 km, atmospheric subsidence (about 2 hPa day^{-1}) spreads at a wide range above 3 km due to the reduced LW emission. Furthermore, the net CRH is dominated by the vertical LW radiative forcing of clouds.
(2) The wind vector variations resulting from the CRH coincide with monsoon circulation, with the positive feedback for wind speeds reaching up to 1.8 and 0.5 m s^{-1} during summer and winter, respectively, while a weakly negative influence (about 0.3 m s^{-1}) occurs at the low-level troposphere below 3 km during winter. Although high clouds, stratiform clouds, and stratocumulus dominate these wind vector variations, deep convective clouds generate the strongest updraft variations (up to 7 m s^{-1}) despite their low occurrence frequency. In summary, the vertical structure of CRH is favourable to the monsoon circulation over East Asia, particularly the summer monsoon circulation.

This study investigates the vertical cloud–radiation associations with the East Asian monsoon circulation on the basis of satellite observations and reanalysis datasets. Our results highlight the considerable impacts of the vertical structure of CRH on the East Asian monsoon circulation by perturbing the vertical atmospheric HRs, irrespective of summer and winter. Moreover, each of the cloud category plays a unique role via their radiative heating/cooling potential and latent heat release within the atmosphere during summer and winter monsoon seasons, respectively. This quantification contributes to understanding the interaction between clouds and monsoon circulation, thereby promoting the evaluation of the impacts of clouds on the Earth–atmosphere system and the assessment of regional climate change in the future.

Acknowledgements

This study is supported by the National Key R&D Program of China (2017YFC0212600 and 2016YFC0200900), the Fundamental Research Funds for the Central Universities (2042017KF0235), and the National Natural Science Foundation of China (41701381 and 41627804). We thank the science teams for providing excellent and accessible CloudSat (www.cloudsat.cira.colostate.edu), CALIPSO (www.eosweb.larc.nasa.gov) and ECMWF (www.ecmwf.int/en/forecasts/datasets) reanalysis datasets.

Disclosure statement

No potential conflict of interest was reported by the authors.

Funding

This study is supported by the National Key R&D Program of China (2017YFC0212600 and 2016YFC0200900), the Fundamental Research Funds for the Central Universities (2042017KF0235), and the National Natural Science Foundation of China (41701381 and 41627804).

References

Bony, S., B. Stevens, D. M. W. Frierson, C. Jakob, M. Kageyama, R. Pincus, T. G. Shepherd, S. C. Sherwood, A. P. Siebesma, and A. H. Sobel. 2015. "Clouds, Circulation and Climate Sensitivity." *Nature Geoscience* 8 (4): 261–268. doi:10.1038/ngeo2398.

Boucher, O., D. Randall, P. Artaxo, C. Bretherton, G. Feingold, P. Forster, and V.-M. Kerminen. 2013. "Clouds and Aerosols." In *Climate Change 2013: The Physical Science Basis. Contribution of Working Group I to the Fifth Assessment Report of the Intergovernmental Panel on Climate Change*, edited by T. F. Stocker, D. Qin, G.-K. Plattner, M. Tignor, S. K. Allen, J. Boschung, A. Nauels, et al., 571–657. Cambridge, UK: Cambridge University Press.

Dee, D. P., S. M. Uppala, A. J. Simmons, P. Berrisford, P. Poli, S. Kobayashi, U. Andrae, M. A. Balmaseda, G. Balsamo, and P. Bauer. 2011. "The ERA-Interim Reanalysis: Configuration and Performance of the Data Assimilation System." *Quarterly Journal of the Royal Meteorological Society* 137 (656): 553–597. doi:10.1002/qj.828.

Ding, Y., and J. C. L. Chan. 2005. "The East Asian Summer Monsoon: An Overview." *Meteorology and Atmospheric Physics* 89 (1–4): 117–142. doi:10.1007/s00703-005-0125-z.

Ding, Y., Y. Liu, S. Liang, X. Ma, Y. Zhang, D. Si, P. Liang, Y. Song, and J. Zhang. 2014. "Interdecadal Variability of the East Asian Winter Monsoon and Its Possible Links to Global Climate Change." *Journal of Meteorological Research* 28: 693–713. doi:10.1007/s13351-014-4046-y.

Ding, Y., Z. Wang, and Y. Sun. 2008. "Inter-decadal Variation of the Summer Precipitation in East China and Its Association with Decreasing Asian Summer Monsoon. Part I: Observed Evidences." *International Journal of Climatology* 28 (9): 1139–1161. doi:10.1002/joc.v28:9.

Fu, Q., and K. N. Liou. 1992. "On the Correlated k-Distribution Method for Radiative Transfer in Nonhomogeneous Atmospheres." *Journal of the Atmospheric Sciences* 49 (22): 2139–2156. doi:10.1175/1520-0469(1992)049<2139:OTCDMF>2.0.CO;2.

Gao, W., C. H. Sui, and Z. Hu. 2014. "A Study of Macrophysical and Microphysical Properties of Warm Clouds over the Northern Hemisphere Using CloudSat/CALIPSO Data." *Journal of Geophysical Research Atmospheres* 119 (6): 3268–3280. doi:10.1002/2013JD020948.

Guo, J., H. Liu, F. Wang, J. Huang, F. Xia, M. Lou, Y. Wu, J. H. Jiang, T. Xie, and Y. Zhaxi. 2016. "Three-dimensional Structure of Aerosol in China: A Perspective from Multi-satellite Observations." *Atmospheric Research S* 178–179 (179): 580–589. doi:10.1016/j.atmosres.2016.05.010.

Guo, Z., and T. Zhou. 2015. "Seasonal Variation and Physical Properties of the Cloud System over Southeastern China Derived from CloudSat Products." *Advances in Atmospheric Sciences* 32 (5): 659–670. doi:10.1007/s00376-014-4070-y.

Guo, Z., T. Zhou, M. Wang, and Y. Qian. 2015. "Impact of Cloud Radiative Heating on East Asian Summer Monsoon Circulation." *Environmental Research Letters* 10 (7): 074014. doi:10.1088/1748-9326/10/7/074014.

Haynes, J. M., T. H. Vonder Haar, T. L'Ecuyer, and D. Henderson. 2013. "Radiative Heating Characteristics of Earth's Cloudy Atmosphere from Vertically Resolved Active Sensors." *Geophysical Research Letters* 40 (3): 624–630. doi:10.1002/grl.50145.

Henderson, D. S., C. D. Kummerow, W. Berg, and D. A. Marks. 2017. "A Regime-Based Evaluation of TRMM Oceanic Precipitation Biases." *Journal of Atmospheric & Oceanic Technology* 34 (12): 2613–2635. doi:10.1175/JTECH-D-16-0244.1.

Henderson, D. S., T. L'Ecuyer, G. Stephens, P. Partain, and M. Sekiguchi. 2013. "A Multisensor Perspective on the Radiative Impacts of Clouds and Aerosols." *Journal of Applied Meteorology & Climatology* 52 (4): 853–871. doi:10.1175/JAMC-D-12-025.1.

Johansson, E., A. Devasthale, T. L'Ecuyer, A. M. L. Ekman, and M. Tjernström. 2015. "The Vertical Structure of Cloud Radiative Heating over the Indian Subcontinent during Summer Monsoon." *Atmospheric Chemistry and Physics* 15 (20): 11557–11570. doi:10.5194/acp-15-11557-2015.

L'Ecuyer, T. S., N. B. Wood, T. Haladay, G. L. Stephens, and P. W. Stackhouse. 2008. "Impact of Clouds on Atmospheric Heating Based on the R04 CloudSat Fluxes and Heating Rates Data Set." *Journal of Geophysical Research Atmospheres* 113 (D8): D00A15.

Li, J., J. Huang, K. Stamnes, T. Wang, Q. Lv, and H. Jin. 2015. "A Global Survey of Cloud Overlap Based on CALIPSO and CloudSat Measurements." *Atmospheric Chemistry and Physics* 15 (1): 519–536. doi:10.5194/acp-15-519-2015.

Li, J., W. C. Wang, X. Dong, and J. Mao. 2017. "Cloud-Radiation-Precipitation Associations over the Asian Monsoon Region: An Observational Analysis." *Climate Dynamics* 49 (9): 3237–3255.

Liu, B., Y. Ma, W. Gong, M. Zhang, W. Wang, and Y. Shi. 2018. "Comparison of AOD from CALIPSO, MODIS, and Sun Photometer under Different Conditions over Central China." *Scientific Reports* 8 (1): 10066. doi:10.1038/s41598-018-28417-7.

Lu, D., Y. Yang, and Y. Fu. 2016. "Interannual Variability of Summer Monsoon Convective and Stratiform Precipitations in East Asia during 1998–2013." *International Journal of Climatology* 36 (10): 3507–3520. doi:10.1002/joc.2016.36.issue-10.

Lu, X., F. Mao, Z. Pan, W. Gong, W. Wang, L. Tian, and S. Fang. 2018. "Three-Dimensional Physical and Optical Characteristics of Aerosols over Central China from Long-Term CALIPSO and HYSPLIT Data." *Remote Sensing* 10 (2): 314. doi:10.3390/rs10020314.

Luo, Y., R. Zhang, and H. Wang. 2009. "Comparing Occurrences and Vertical Structures of Hydrometeors between Eastern China and the Indian Monsoon Region Using CloudSat/CALIPSO Data." *Journal of Climate* 22 (4): 1052–1064. doi:10.1175/2008JCLI2606.1.

Mace, G. G., and Q. Zhang. 2014. "The CloudSat Radar-lidar Geometrical Profile Product (rl-geoprof): Updates, Improvements, and Selected Results." *Journal of Geophysical Research: Atmospheres* 119 (15): 9441–9462.

Mace, G. G., Q. Zhang, M. Vaughan, R. Marchand, G. Stephens, C. Trepte, and D. Winker. 2009. "A Description of Hydrometeor Layer Occurrence Statistics Derived from the First Year of Merged CloudSat and CALIPSO Data." *Journal of Geophysical Research: Atmospheres* 114 (D8): 414–416. doi:10.1029/2007JD009755.

Mao, F., Z. Pan, D. S. Henderson, W. Wang, and W. Gong. 2018. "Vertically Resolved Physical and Radiative Response of Ice Clouds to Aerosols during the Indian Summer Monsoon Season." *Remote Sensing of Environment* 216: 171–182. doi:10.1016/j.rse.2018.06.027.

Mather, J. H., S. A. McFarlane, M. A. Miller, and K. L. Johnson. 2007. "Cloud Properties and Associated Radiative Heating Rates in the Tropical Western Pacific." *Journal of Geophysical Research: Atmospheres* 112 (D5). doi:10.1029/2006JD007555.

Pan, Z., W. Gong, F. Mao, J. Li, W. Wang, C. Li, and Q. Min. 2015. "Macrophysical and Optical Properties of Clouds over East Asia Measured by CALIPSO." *Journal of Geophysical Research: Atmospheres* 120 (22): 11653–11668. doi:10.1002/2015JD023735.

Pan, Z., F. Mao, W. Gong, Q. Min, and W. Wang. 2017. "The Warming of Tibetan Plateau Enhanced by 3D Variation of Low-level Clouds during Daytime." *Remote Sensing of Environment* 198: 363–368. doi:10.1016/j.rse.2017.06.024.

Pan, Z., F. Mao, W. Wang, T. Logan, and J. Hong. 2018. "Examining Intrinsic Aerosol-Cloud Interactions in South Asia through Multiple Satellite Observations." *Journal of Geophysical Research: Atmospheres* 123 (19): 11–210. doi:10.1029/2017JD028232.

Quaas, J., O. Boucher, N. Bellouin, and S. Kinne. 2008. "Satellite-based Estimate of the Direct and Indirect Aerosol Climate Forcing." *Journal of Geophysical Research: Atmospheres* 113 (D5): 79–88. doi:10.1029/2007JD008962.

Rodwell, M. J., and B. J. Hoskins. 2001. "Subtropical Anticyclones and Summer Monsoons." *Journal of Climate* 14 (15): 3192–3211. doi:10.1175/1520-0442(2001)014<3192:SAASM>2.0.CO;2.

Rosenfeld, D., M. O. Andreae, A. Asmi, M. Chin, G. Leeuw, D. P. Donovan, R. Kahn, S. Kinne, N. Kivekäs, and M. Kulmala. 2014. "Global Observations of Aerosol-Cloud-Precipitation-Climate Interactions." *Reviews of Geophysics* 52 (4): 750–808.

Sassen, K., Z. Wang, and D. Liu. 2008. "Global Distribution of Cirrus Clouds from CloudSat/Cloud-Aerosol Lidar and Infrared Pathfinder Satellite Observations (CALIPSO) Measurements." *Journal of Geophysical Research: Atmospheres* 113 (D8): 347–348. doi:10.1029/2008JD009972.

Sassen, K., Z. Wang, and D. Liu. 2009. "Cirrus Clouds and Deep Convection in the Tropics: Insights from CALIPSO and CloudSat." *Journal of Geophysical Research* 114 (114): 6149–6150. doi:10.1029/2009JD011916.

Stephens, G. L., D. G. Vane, S. Tanelli, E. Im, S. Durden, M. Rokey, D. Reinke, P. Partain, G. G. Mace, and R. Austin. 2008. "CloudSat Mission: Performance and Early Science after the First Year of Operation." *Journal of Geophysical Research: Atmospheres (1984–2012)* 113 (D8). doi:10.1029/2008JD009982.

Wang, B., J. Liu, H.-J. Kim, P. J. Webster, and S.-Y. Yim. 2012. "Recent Change of the Global Monsoon Precipitation (1979–2008)." *Climate Dynamics* 39 (5): 1123–1135. doi:10.1007/s00382-011-1266-z.

Wang, Y., and C. Wang. 2016. "Features of Clouds and Convection during the Pre- and Post-onset Periods of the Asian Summer Monsoon." *Theoretical and Applied Climatology* 123 (3–4): 551–564. doi:10.1007/s00704-015-1372-7.

Winker, D. M., W. H. Hunt, and M. J. McGill. 2007. "Initial Performance Assessment of CALIOP." *Geophysical Research Letters* 34 (19): 228–262. doi:10.1029/2007GL030135.

Winker, D. M., J. Pelon, J. A. Coakley, S. A. Ackerman, R. J. Charlson, P. R. Colarco, P. Flamant, Q. Fu, R. M. Hoff, and C. Kittaka. 2010. "The CALIPSO Mission: A Global 3D View of Aerosols and Clouds." *Bulletin of the American Meteorological Society* 91 (9): 1211–1230. doi:10.1175/2010BAMS3009.1.

Wu, G., B. He, Y. Liu, Q. Bao, and R. Ren. 2015. "Location and Variation of the Summertime Upper-troposphere Temperature Maximum over South Asia." *Climate Dynamics* 45 (9–10): 2757–2774. doi:10.1007/s00382-015-2506-4.

Zuluaga, M. D., C. D. Hoyos, and P. J. Webster. 2010. "Spatial and Temporal Distribution of Latent Heating in the South Asian Monsoon Region." *Journal of Climate* 23 (8): 2010–2029. doi:10.1175/2009jcli3026.1.